

A Viable Hydrogen Storage and Release System Based on Cesium Formate and Bicarbonate Salts: Mechanistic Insights into the Hydrogen Release Step

Katerina Sordakis, Andrew F. Dalebrook, and Gábor Laurenczy*^[a]

Aqueous solutions of cesium formate and bicarbonate represent an effective hydrogen storage–delivery couple that undergoes either release or take up of hydrogen in the presence of $\{\text{RuCl}_2(m\text{TPPTS})_2\}_2$ (TPPTS = triphenylphosphine trisulfonate) and excess *m*TPPTS ligand, with no other additives required. Cesium salt solutions offer the advantage of improved volumetric and gravimetric H_2 density compared to their sodium and potassium analogs, owing to their high water solubility. Details of the equilibrium between formate and bicarbonate, which constitutes an important parameter for the applicability of this H_2 storage/release cycle, were determined. H_2 produc-

tion is readily tunable by controlling the operating pressure. This behavior was also rationalized through the identification of catalytic intermediates under various conditions. High concentration formate and bicarbonate solutions were used during the tests and the bidirectional catalytic system could be recycled without loss of activity or replacement of solvent. A tentative mechanism is proposed for the formate dehydrogenation step. Among the identified hydride species, the penta-coordinated $[\text{RuH}(\text{H}_2\text{O})(\text{TPPTS})_3]$ complex was indispensable for promoting the formate dehydrogenation reaction.

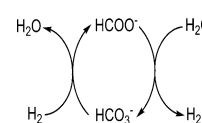
Introduction

Hydrogen is regarded as one of the most promising future energy vectors from both an environmental as well as a socio-economic point of view, due to its potentially clean production and utilization pathways, attractive inherent fuel properties and most importantly its borderless availability.^[1] One crucial milestone towards the successful introduction of hydrogen systems into our current energy infrastructure and potentially long-term energy supply security will require demonstrable assurances that hydrogen installations are inherently safe. In the frame of a transition towards more innovative and sustainable energy strategies, which is becoming inevitable and all the more pressing, rapid steps for the implementation of a hydrogen economy have been realized.^[2] However some of the main aspects, namely hydrogen storage and handling, still remain without adequately satisfying solutions in terms of energy and cost efficiency as well as safety.

The utilization of carbon dioxide in energy storage was first suggested by Williams et al. in the late 1970s,^[3] followed by Wiener et al.^[4] who proposed formate and bicarbonate salts as chemical hydrogen carriers. The chemical equilibria in various formate–bicarbonate salt systems (Scheme 1) in the presence of a heterogeneous catalyst were later investigated by Engel et al.^[5] However it was only recently that formic acid (FA) was revisited as a liquid hydrogen carrier and these systems once more attracted attention for hydrogen storage.^[6,7]

Similarly to FA, aqueous solutions of formate and bicarbonate are easily and safely stored and transported, owing to their liquid nature and very low toxicity. The utilization of water as a solvent adds to the straightforward, cost-effective, and “green” nature of this hydrogen storage system. Furthermore alkali metal salts release hydrogen in the absence of additional gaseous coproducts, that is, CO_2 , which has benefits for flow processes.

The utilization of the greenhouse gas CO_2 as a C_1 building block through its homogenous reduction in an alkaline environment has been widely studied^[8–13] as well as homogenous formic acid decomposition for hydrogen storage applications.^[14,15] However, the similar bicarbonate hydrogenation reaction^[16–21] and, more significantly, its interconnection with the formate dehydrogenation reaction remain largely unexplored.^[22–24] Interestingly most published reports focused on sodium and potassium salts as hydrogen carriers while the cesium salts were largely neglected, possibly owing to their decreased gravimetric hydrogen density (larger atomic weight of the metal cation) as well as the lower natural abundance of cesium metal.^[25] However, the former can be largely counterbalanced by the increased water solubility of the cesium salts as discussed in detail below. One of the few studies on hydrogen release from cesium salts was published by Onsager et al., who postulated that formate salts derived from carbon monoxide and different carbonates were potential intermediates for hydrogen production.^[26]



Scheme 1. Hydrogen storage and release based on the formate/bicarbonate cycle.

[a] K. Sordakis, A. F. Dalebrook, Prof. Dr. G. Laurenczy
EPFL ISIC, LCOM
1015 Lausanne (Switzerland)
E-mail: gabor.laurenczy@epfl.ch

Supporting information for this article is available on the WWW under <http://dx.doi.org/10.1002/cctc.201500359>.

Results and Discussion

Evaluation of cesium formate and bicarbonate salts for H₂ storage

The applicability of such a hydrogen storage system strongly depends on both the maximum solubility and the conversion of the substrates under the specific reaction conditions. In this sense, cesium salts clearly offer an advantage over their sodium and potassium analogues owing to their increased water solubility, resulting in a higher volumetric and gravimetric hydrogen content. Since alkali metal formate salts have higher water solubility than the corresponding bicarbonate salts, the solubility of the latter is the limiting factor. Considering that the solubility of cesium bicarbonate (209.0 g/100 g_{H₂O} at 15 °C) is more than twenty and five times higher than the solubilities of the respective sodium (10.3 g/100 g_{H₂O} at 25 °C) and potassium salts (36.2 g/100 g_{H₂O} at 25 °C),^[27] cesium salts stand out for possible practical applications. At 15 °C a saturated aqueous solution of CsHCO₃ (and consequently CsOOCH) has a concentration (storage capacity) of approximately 11 mol kg⁻¹ H₂O and a volumetric H₂ density of 14 g L⁻¹ (the solution volume increases approximately 57% upon addition of the solute). It is however important to point out that this value can be significantly increased at elevated temperatures, which is relevant for stationary applications for which the installation of a heating system is straightforward. For reference, the solubility of CsOOCH in 100 g H₂O increases to 2012.0 g at 95 °C.^[28] However it must be noted that such a saturated solution cannot be used for hydrogen storage systems because water becomes the limiting reactant during formate dehydrogenation. Using the maximal CsOOCH concentration of 18 mol kg_{water}⁻¹, our system has a gravimetric hydrogen storage capacity of 0.85 wt% at 80 °C and a volumetric H₂ density of 23 g L_{solution}⁻¹.

Toxicity

A considerable parameter for practical hydrogen storage applications is the impact of a system failure on both human health and the environment. As cesium salts have never been reported as hydrogen carriers, a short insight into their properties is pertinent. The cesium ion itself is more toxic than sodium, but less toxic than the potassium or lithium ion.^[29] However, the toxicity of alkali metal salts is strongly influenced by the particular anion. As cesium formate has widely replaced the toxic and corrosive zinc bromide as a drilling and completion fluid in the oil industry,^[30] it has undergone extensive studies into its biochemical compatibility, toxicology and environmental impacts. Cesium formate is readily biodegradable,^[31] it is characterized as an environmental-friendly compound and an accidental release is not expected to adversely affect the environment owing to the well-known formate degradation pathways. Furthermore, elevated cesium levels in the environment have not been reported to cause any adverse effects.^[32,33] The discharge of cesium in aquatic systems is likely to be extenuated by dilution, whereas in terrestrial environments sorption of

cesium would minimize its bioavailability. Cesium formate is not a reported carcinogen but is known to be a mild eye and skin irritant. Chronic health effects are mainly associated with high repeated oral doses of the compound which are highly unlikely to be a significant factor with small- to medium-scale hydrogen storage systems. Cesium bicarbonate has not been as extensively studied and therefore far less data is available. It is classified as a non-hazardous material according to European standards. The bicarbonate ion itself has a wide natural occurrence as part of the photosynthetic mechanism of plants as well as the CO₂-water equilibria. Its toxicity is mainly associated to an increase in the pH of water bodies through the aqueous bicarbonate-carbonate equilibrium.

Catalyst and system optimization

We are interested in a catalytic system active for both formate dehydrogenation and bicarbonate hydrogenation. In this way catalyst removal and replacement (depending on the reaction of interest) is avoided, which would otherwise pose a significant burden on the development of rechargeable "H₂ batteries". However, any catalytic system active for both reactions would tend towards an equilibrium position (Scheme 1). Data on this phenomenon would be crucial for controlling the charging (H₂ storage) and discharging (H₂ release) steps in continuous processes. Herein we report for the first time an attempt to produce hydrogen for practical applications, by substantially increasing the substrate concentration and consequently volumetric H₂ density, owing to the very high water solubility of cesium formate.

The reverse hydrogenation reaction of dilute NaHCO₃ solutions by an in situ formed {RuCl₂(*m*TPPMS)₂}₂ + *m*TPPMS catalyst (TPPMS = triphenylphosphine monosulfonate) was previously studied as part of a charge-discharge device.^[22] Here we report a similar system making use of the trisulfonated analog {RuCl₂(*m*TPPTS)₂}₂ + 2 *m*TPPTS (1) (TPPTS = triphenylphosphine trisulfonate) with increased water solubility (1100 g L⁻¹ *m*TPPTS vs. 28 g L⁻¹ *m*TPPMS) and hence catalytic concentration. NaO¹³CH and CsOOCH were chosen as substrates for dehydrogenation, the former being isotopically enriched to enhance NMR detection at low concentrations. Initially, the stability and activity of the catalytic system over extended time periods at elevated temperatures were optimized by varying the metal-to-excess-phosphine ratio. The highest rate for formate dehydrogenation as well as prolonged catalytic lifetime (Figure 1, blue squares) was obtained with a twofold excess of *m*TPPTS per ruthenium dimer (that is, total Ru/P = 1:3). With lower excesses, the initial rate for formate dehydrogenation was equally high (Figure 1, red squares), but gradually decreased with the concurrent appearance of black ruthenium nanoparticles within the reaction solution. It is known that insufficient phosphine stoichiometry leads to poor stabilization at ruthenium, which is also likely in this case.^[34] On the contrary, with larger excesses of *m*TPPTS the first coordination sphere of the metal becomes saturated. This would hinder substrate coordination and thus inhibit formate dehydrogenation at higher Ru/P ratios.

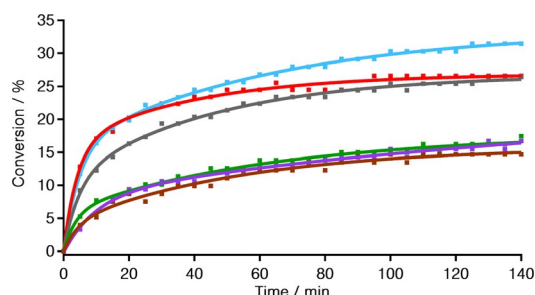


Figure 1. Ru/excess phosphine ratio effect on 2 mol kg⁻¹ aqueous cesium formate dehydrogenation reaction applying 10 mmol kg⁻¹ Ru at 80 °C. ■ 1:1; ● 1:2, ▲ 1:4, ◆ 1:8, ▼ 1:10, ▾ 1:15.

Table 1. Catalytic dehydrogenation of formate salts in the presence of (1).^[a]

Entry	MOOCH [mol kg ⁻¹]	Ru [mol kg ⁻¹]	Conversion ^[d] [%]	Time [h]	Conditions
1	0.24 ^[b]	0.01	80	3	isobaric (1 bar)
2	0.24 ^[b]	0.02	60	1.5	isobaric (1 bar)
3 ^[e]	0.24 ^[b]	0.02	86	1.5	isobaric (1 bar)
4	2 ^[c]	0.01	30	1	isochoric
5	3 ^[c]	0.01	25	10	isochoric
6	5 ^[c]	0.01	25	11	isochoric
7	10 ^[c]	0.1	23	3	isochoric
8	15 ^[c]	0.16	20	2	isochoric
9 ^[f]	15 ^[c]	0.16	10.7	3	isochoric
10 ^[g]	15 ^[c]	0.16	6.5	3	isochoric

[a] Experimental conditions: Ru/excess phosphine = 1:2, $T = 80^\circ\text{C}$, 2 mL H₂O. [b] M = Na, ¹³C-enriched NaOO¹³CH was used. [c] M = Cs. [d] The conversion was calculated from ratio HCOO⁻/HCO₃⁻ determined by quantitative ¹³C NMR spectroscopy.^[41] [e] With stirring. [f] Pressurized with 25 bar H₂. [g] Pressurized with 50 bar H₂. Reproducibility of experiments is $\pm 5\%$.

Heating a solution of 0.24 mol kg⁻¹ aqueous NaOO¹³CH at 80 °C in the presence of (1) under a slight overpressure of N₂, for which the outlet was vented by means of a needle punctured through a rubber septum, resulted in 80% conversion of formate to bicarbonate within 3 h (Table 1, entry 1). The rate of the reaction decreased with decreasing substrate concentration (Figure 2, black squares), although the final conversion reached 100%. When the reaction solution was stirred to accel-

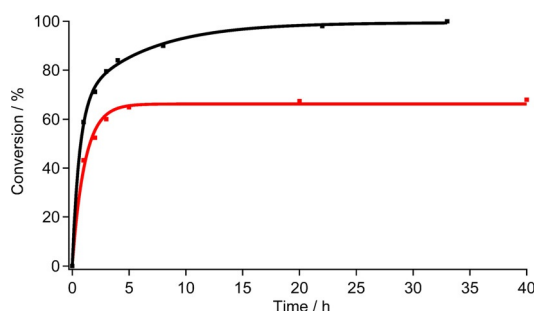


Figure 2. Rate of 0.24 mol kg⁻¹ aqueous sodium formate (NaOO¹³CH) dehydrogenation reaction applying 10 mmol kg⁻¹ Ru and 2 equiv. mTPPTS at 80 °C, under small N₂ overpressure (■) and under isochoric conditions (■).

erate removal of the produced H₂ gas, conversion improved from 60 to 86% within 1.5 h (Table 1, entries 2 and 3).

Subsequently we examined the catalytic performance of (1) under isochoric conditions, that is, without releasing the produced H₂ gas from the reaction solution. In this case the sodium formate conversion levelled off at 63% (Figure 2, red squares) indicating the substantial influence of even minimal amounts of H₂ on the reaction and the presence of a thermodynamic equilibrium in the formate–bicarbonate system. In this case, the calculated turnover frequency (TOF) for the first hour was 10 h⁻¹. Similar behavior was earlier reported for a FA/NEt₃ system at equilibrium in the presence of a {RuCl₂(benzene)}₂ + 1,2-bis(diphenyl-phosphino)ethane pre-catalyst.^[35] Beller et al. also reported that potassium formate decomposition is unfavorable at elevated H₂ pressures with a ruthenium pincer catalyst.^[36] Similarly, formic acid dehydrogenation was inhibited by moderate H₂ pressures in the presence of an Fe(BF₄)₂ metal precursor and tris[(2-diphenylphosphino)ethyl]phosphine ligand.^[37] In the current catalytic system, pressurization of a 15 mol kg⁻¹ CsOOCH solution to 25 or 50 bar H₂ with subsequent heating of the mixture decreased the obtained conversions from 20.0 to 10.7 and 6.5%, respectively (Table 1, entries 8–10). However formate decomposition restarted after the release of pressure.

Under isochoric conditions, a stepwise increase in the concentration of cesium formate revealed a trend of decreasing final conversions with increasing H₂ pressures (Table 1, entries 4–8), even though a larger total quantity of H₂ was produced. The rate of formate dehydrogenation improved with increasing pre-catalyst concentration but the equilibrium position was also attained faster. Therefore the conversion obtained after the first five minutes of reaction was used for comparison (Figure S1 in the Supporting Information). Catalyst concentrations of up to 0.24 mol/kg were tested and correlated with a constant increase in the observed activity; however higher concentrations were impractical due to significant increases of viscosity.

The same catalytic system (1) was also tested for its activity in the bicarbonate hydrogenation reaction under similar reaction conditions. A 0.24 mol kg⁻¹ aqueous NaH¹³CO₃ solution was pressurized with 100 bar H₂, for which conversions of 96% and 98% were attained within 1 and 2 h, respectively (Table 2, entry 1). This corresponds to a TOF of approximately 23 h⁻¹ for the first hour (vs. 10 h⁻¹ for the formate dehydrogenation reaction), implying that (1) is more active for bicarbonate hydrogenation. Also in this case we investigated the effect of increasing substrate concentration (entries 2, 5–8). Lowering the initial H₂ pressure from 100 to 50 bar decreased the reaction rate, resulting in overall conversions of 28 and 14%, respectively, within 3 h (entries 3, 4).

We also studied the effect of different counterions (Cs, Na, and K) of formate and bicarbonate solutions (Table S1 in the Supporting Information). In contrast to previously published results,^[23,36] there were no differences in either conversion efficiencies or reaction rates. For example, both NaOOCH and CsOOCH were dehydrogenated with 30% conversion in 1 h (Table S1 in the Supporting Information) and comparative

Entry	MHCO ₃ [mol kg ⁻¹]	Ru [mol kg ⁻¹]	Conversion ^[d] [%]	Time [h]
1	0.24 ^[b]	0.01	96; > 98	1; 2
2	2 ^[c]	0.02	80	20
3	2 ^[c]	0.02	28	3
4 ^[e]	2 ^[c]	0.02	14	3
5	3 ^[c]	0.01	80	40
6	5 ^[c]	0.01	80	120
7	10 ^[c]	0.1	80	84
8	15 ^[c]	0.1	80	96

[a] Experimental conditions: Ru/excess phosphine = 1:2, T = 80 °C, 2 mL H₂O, P(H₂)_{init} = 100 bar. [b] M = Na, ¹³C-enriched NaHCO₃ was used. [c] M = Cs. [d] The conversion was determined by quantitative ¹³C NMR spectroscopy.^[41] [e] Pressurization with 50 bar H₂. Reproducibility of experiments is ± 5%.

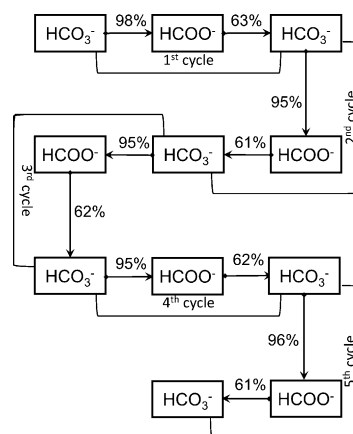
experiments for bicarbonate hydrogenation were equally similar. This is to be expected if the salts are fully dissociated in solution and counterions only play a spectator role. However, highly concentrated solutions of cesium formate and bicarbonate are significantly more viscous. In these situations mass-transfer limitations may come into play, but comparisons cannot be made with the less soluble sodium and potassium analogues.

Finally, we evaluated the catalytic activity and stability in consecutive H₂ storage and release cycles. Consistent conversions for both the bicarbonate hydrogenation and the formate decomposition reactions were obtained in four recycling experiments. Initially, an aqueous solution of bicarbonate was pressurized with 100 bar H₂ and left to equilibrate at 80 °C, resulting in an overall conversion of 98%. Subsequently the excess gas was released and the solution reheated under isochoric conditions, resulting in a formate dehydrogenation yield of 63%. Notably, the removal of solvent and/or replacement of catalyst were not necessary and the CO₂-like hydrogen carrier remained in the reaction mixture. The same closed cycle was repeated five times without any loss of catalytic activity or aerobic degradation. In these experiments, the readily available NaOO¹³CH was utilized for convenience (Scheme 2).

Mechanistic investigations

We have already investigated related catalytic cycles derived from RuCl₃·H₂O + mTPPTS systems under acidic conditions.^[34,38] Here we present results of mechanistic investigations on (1), albeit in a basic environment and with a higher excess of the phosphine ligand. Depending on the applied conditions multiple hydride species were identified in solution.

When ¹³C enriched NaOO¹³CH was added to an aqueous solution of (1), a doublet resonance was detected in the ¹³C NMR spectrum at 175.8 ppm (*J*_{H-C} = 207 Hz), attributed to the previously identified complex *trans*-[Ru(OOCH)(H₂O)₃(TPPTS)₂] (2).^[34] The ³¹P NMR signal of this complex at 55.9 ppm^[39] could not be clearly distinguished as it overlapped with another peak at 56.5 ppm, which is expected upon formation of the pentacoor-



Scheme 2. Conversions obtained during consecutive bicarbonate hydrogenation formate dehydrogenation cycles.

inated 16-electron complex *trans*-[Ru(H₂O)₂(TPPTS)₃] (3).^[39,40] (Figure 3)

Upon heating the same solution at 80 °C, signals for complex (2) disappeared from NMR spectra and multiple hydride species appeared in the ¹H NMR spectrum.

This could rationalize facile conversion of formate to bicarbonate. At the beginning of the reaction, the main hydride species were identified at -18.8 (quartet) and -12.0 ppm (pseudo quartet) and as two broad singlets at -8.5 ppm and -20.7 ppm, all of which collapsed into singlets if ³¹P decoupled. The quartet at -18.8 ppm in the ¹H NMR (*J*_{H-P} = 25.5 Hz) and 57.4 ppm in the ³¹P NMR spectrum was previously attributed to (4) (Figure 4)^[40] and identified as

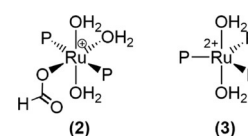


Figure 3. Structures of complexes (2) and (3).

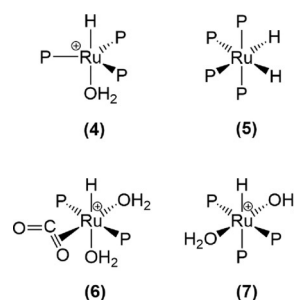


Figure 4. Structures of complexes (4)–(7).

an active catalyst in the hydrogenation of olefins.^[41] The highly reactive nature of coordinatively unsaturated divalent ruthenium complexes with formal 16 electron counts prompted us to further certify the assigned structure of (4) by fitting of the respective ¹H NMR spectrum with NMRICMA on Matlab software.^[42] The coupling constants calculated for different coupling modes were in all cases identical, indicating that the three phosphorus ligands in (4) are chemically and magnetically equivalent – unequivocally confirming a trigonal bipyramidal

molecular geometry (Figure S2 in the Supporting Information). Basset et al. reported that in aqueous solutions and under low H_2 pressures, (3) converts into (4), which is in equilibrium with $[RuHCl(H_2O)(TPPTS)_2]$ (4b).^[40] This latter species could thus give rise to the broad signal observed at -20.7 ppm in the 1H NMR spectrum (ratio (4)/(4b)=1:0.2). The signal at -12.0 ppm became more pronounced at slightly higher H_2 pressures and was attributed to $[RuH_2(mTPPTS)_4]$ (5) ($J_{H-P}=35$ Hz), which was reported to form from $\{RuCl_2(mTPPTS)_2\}_2$ and excess phosphine under basic conditions and at elevated H_2 pressures.^[39,43] The two hydride ligands in (5), even though chemically equivalent, are magnetically distinct and thus form part of an AAX'Y₂ spin system, in which X and Y are equatorial and axial ^{31}P nuclei respectively. These hydrides split into a pseudo-quartet in the 1H NMR spectrum and collapse into a singlet upon ^{31}P decoupling (Figure S7 in the Supporting Information). After further heating of the reaction solution at $80^\circ C$ for 30 min, a triplet of doublets at -16.3 ppm and a doublet of triplets at -10.2 ppm appeared in the 1H NMR spectrum. The former species was stable for at least 48 h at $80^\circ C$ and collapsed into a triplet when ^{13}C decoupled ($J_{H-P}=20$ Hz) and a doublet when ^{31}P decoupled ($J_{H-C}=10$ Hz) (Figure 5). The corresponding ^{31}P and ^{13}C signals were found at 44.1 and 204.9 ppm respectively. This complex (6) was previously characterized^[34] and reported to be part of the slow cycle in a formic acid decomposition reaction in the presence of NaOOCH. However, in that case coordination of formic acid on (6) was a prerequisite for the catalytic cycle to progress. As in the current system we do not expect

formic acid to be present in solution at any stage of the reaction (pH is kept in the basic range), it is likely that (6) is a "dead-end" species, that is, it is formed without taking part in the catalytic mechanism presented below. The doublet of triplets at -10.2 ppm collapsed into a singlet when ^{31}P decoupled ($J_{H-Trans}=73$ Hz, $J_{H-Cis}=28$ Hz) and could have the structure of (7) as the *mer* complex (Figure 4). Upon measuring the spin-lattice relaxation time ($T_1=359$ ms) of this hitherto unknown compound, it was confirmed to contain discrete hydrides as opposed to a dihydrogen ligand.^[44]

During the initial fast dehydrogenation of formate to bicarbonate, a hydride signal for (4) and a second broad singlet at -8.5 ppm (4c) were present as the main resonances in the 1H NMR spectrum. Several attempts to obtain further information on the multiplicity of the latter peak by NMR spectroscopy failed. However the spin-lattice relaxation time of this peak was measured as 33 ms, indicating that it is likely to represent a non-classical dihydrogen ligand. After 90 min heating, the peak intensities of (4) and (4c) decreased while that of (7) increased, and a new, broad peak at -8.2 ppm appeared. After prolonged heating, this peak resolved as a pseudo-quartet with $J_{H-P}\approx 23.5$ Hz—in reality a doublet of triplets with similar coupling constants. If ^{13}C enriched NaOO ^{13}C H was used, the splitting became more complicated and the peak appeared as a pseudo-quintet (Figure S10, left, in the Supporting Information). $^1H\{^{31}P\}$ and $^1H\{^{13}C\}$ decoupling experiments gave rise to doublet and quartet signals, respectively ($J_{H-P}=23.5$ Hz, $J_{H-C}=17.5$ Hz, Figures S9 and S10 in the Supporting Information).

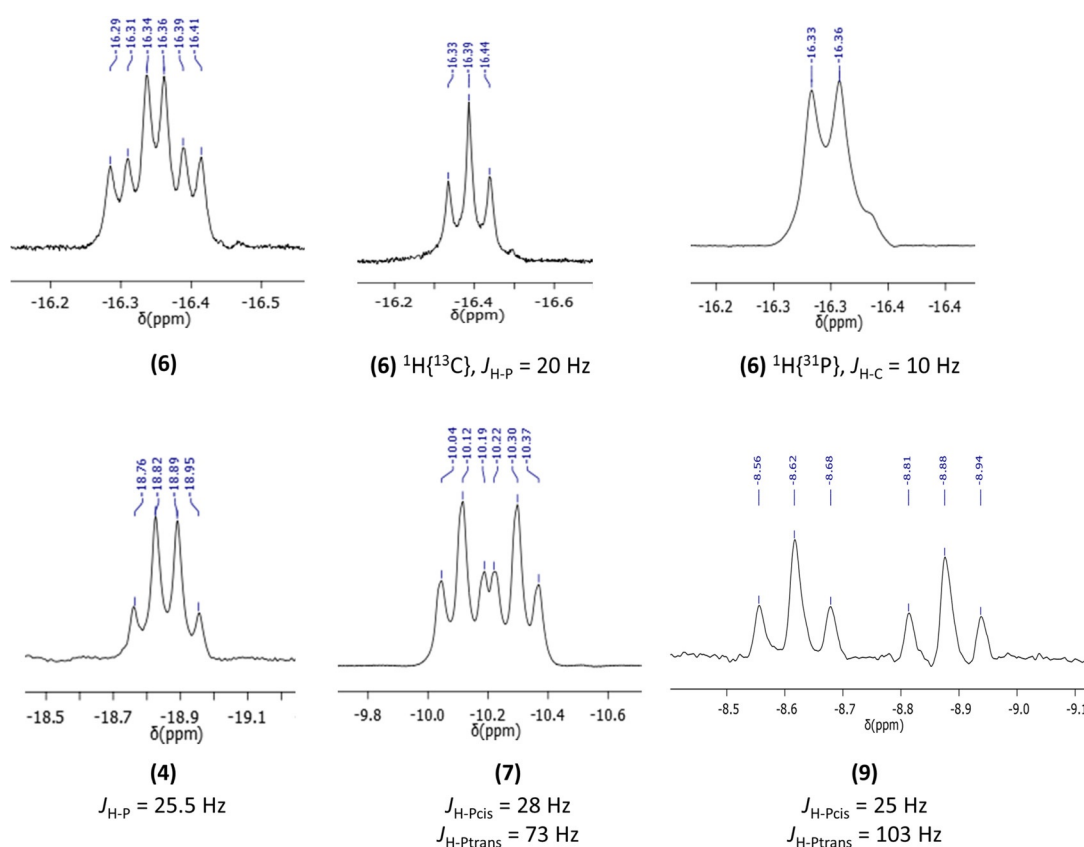


Figure 5. 1H NMR spectra of complexes (4), (6), (7), and (9) with enhanced signal/noise ratio.^[45]

Similar coupling constants were obtained by fitting the pseudo-quintet signal with NMRICMA on Matlab ($J_{H-Pa} = 27.4$ Hz, $J_{H-Pb} = 21.4$ Hz, $J_{H-C} = 17.8$ Hz). In the ^{13}C NMR spectrum, a singlet was detected at 205.4 ppm. The similar values obtained for the coupling constants indicate that a *mer* phosphine hydride species with one $\eta^2\text{-CO}_2$ ligand, (**8**) was present in solution. The pseudo-quintet peak characteristic of (**8**), in reality

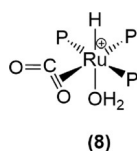


Figure 6. Structure of complex (**8**).

comprised of a doublet of triplets, can be justified by the similar values of the coupling constants for the various ligands. (Figure 6)

As mentioned, H_2 gas can significantly decrease the catalytic activity. Therefore we examined the formation of hydride species under 60 bar H_2 by NMR techniques. In this case all the above mentioned

species were detected with the exception of (**4**) and (**4b**), which were not present at any stage of the reaction. Under this pressure, the conversion of formate was limited to 2%, indicating that the formation of (**4**) is vital to progress through the catalytic mechanism. The presence of an equilibrium between (**4**) and the dihydrogen-hydride complex (**4c**) could explain the observed behavior. Even though the ruthenium-hydrogen interaction in (**4c**) is weaker than the iron-hydrogen interaction in the related Fe- H_2 complex, stable species of the former type were isolated and their crystal structures reported.^[46] If pressure was released and the reaction solution heated, sodium formate was successfully dehydrogenated to bicarbonate with the concomitant formation of complex (**4**), as confirmed by ^1H NMR spectroscopy. If the formate dehydrogenation was performed under a protective N_2 atmosphere and the produced H_2 gas vented throughout, (**4**) was present in solution throughout the reaction, explaining the full conversion obtained.

Under elevated H_2 pressures, a ^1H NMR spectrum of the reaction mixture also contained a doublet of triplets at -8.7 ppm, which collapsed to a singlet if ^{31}P decoupled ($J_{H-Prans} = 103$ Hz, $J_{H-Pcis} = 25$ Hz). Simultaneously, a peak at 204.2 ppm was present in the ^{13}C NMR spectrum. Previously a species with similar

characteristics (^1H NMR $\delta = -8.08$ ppm, $J_{H-Prans} = 107.9$ Hz, $J_{H-Pcis} = 23.8$ Hz) was reported to have the structure of (**9**).^[38] (Figure 7)

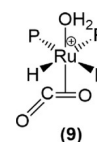


Figure 7. Structure of complex (**9**).

To verify the presence of the coordinated $\eta^2\text{-CO}_2$ ligand, ^{13}C enriched $\text{NaOO}^{13}\text{CH}$ was utilized. In this case (**9**) gave rise to a pseudo-doublet of quartets in the ^1H NMR spectrum (Figure S12 in the Supporting Information), indicating that the coupling constants J_{H-Pcis} and J_{H-C} are in a similar range. $^1\text{H}\{^{31}\text{P}\}$ spectra contained a broad singlet at -8.8 ppm in the ^1H NMR spectrum (the splitting due to ^{13}C coupling was not resolved). This information supports our hypothesis regarding the assigned structure of (**9**).

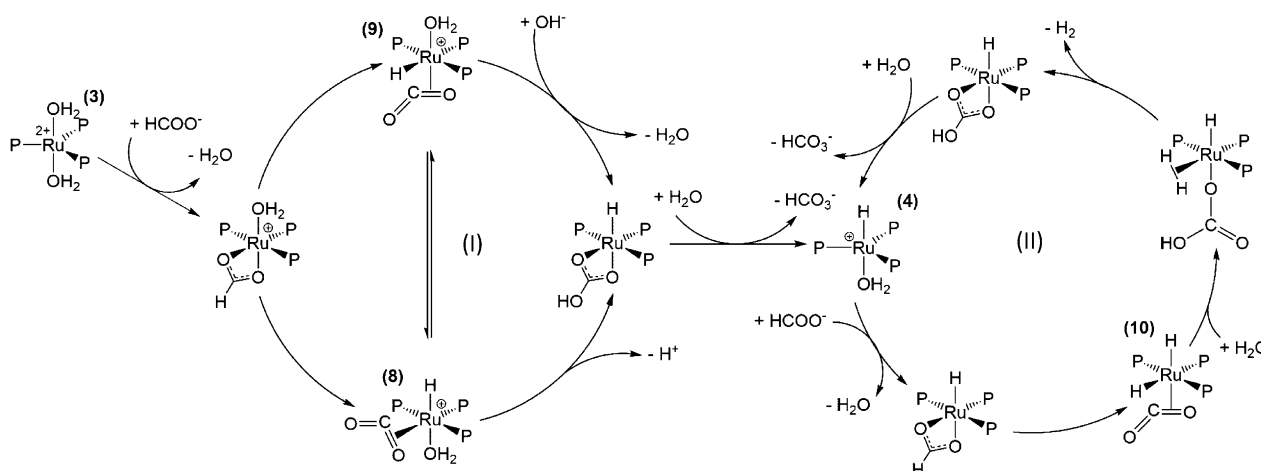
No coordinated bicarbonate species were detected by ^{13}C NMR spectrometry, as it is likely that signals for this species are coincident with the large formate resonance^[17] (170.5 ppm in the ^{13}C NMR for a $[\text{Ru}(\text{HCO}_3)_2(\text{mTPPMS})_2]$ complex).

Mechanism

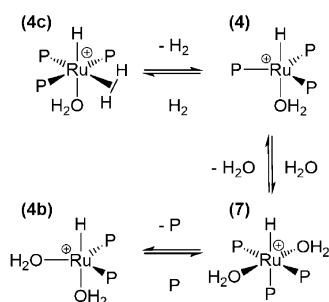
During our investigations, several previously known as well as new hydride species were identified in solution. A tentative mechanism which correlates these catalytic species with the macroscopic behavior exhibited during the formate decomposition reaction is given in Scheme 3.

When $[\text{RuCl}_2(\text{mTPPTS})_2]_2$ is dissolved in water in the presence of excess *m*TPPTS, *trans*- $[\text{Ru}(\text{H}_2\text{O})_2(\text{TPPTS})_3]$ (**3**) is formed. As H_2 gas is not present at the beginning of the reaction, the trigonal-bipyramid hydride complex (**4**) should be formed via HCOO^- coordination on (**3**), followed by β -hydride elimination which leads to the formation of isomers (**8**) and (**9**). The coordinated $\eta^2\text{-CO}_2$ ligand may then rearrange to a bidentate bicarbonate by interaction with water, yielding a $[\text{RuH}(\text{HCO}_3)(\text{TPPTS})_3]$ complex. Release of the bicarbonate ligand leads to formation of (**4**), which participates in various equilibria (Scheme 4).

Coordination of a water ligand to (**4**) gives the octahedral complex (**7**), which may then yield complex (**4b**) via loss of a TPPTS ligand. The presence of an equilibrium between (**4**)



Scheme 3. Proposed catalytic mechanism for formate dehydrogenation, P = *m*TPPTS $^{3-}$.



Scheme 4. Equilibria between species (4), (4b), (4c), and (7), P = *m*TPPTS³⁻.

and (4c) could explain the inhibition of catalytic activity under elevated H₂ pressure, which would favor the formation of (4c) and consequently hinder the progression to cycle (II).

Complex (4) may then enter cycle (II) via coordination of a formate ligand, followed by a β -hydride elimination step, which affords a non-classical dihydride complex (10) (not observed during the reaction). Reaction of the coordinated η^2 -CO₂ ligand of (10) with water leads to a species with both H₂ and HCO₃⁻ ligands, the successive elimination of which regenerates complex (4). Protonation of (4) and subsequent H₂ elimination is also a possible pathway to complex (3).

Conclusions

The interconnection of bicarbonate hydrogenation and formate decomposition reactions in aqueous media without any further additives truly offers a way towards a practical and rechargeable hydrogen battery. Electron-rich and coordinatively unsaturated Ru^{II} *m*TPPTS complexes with three phosphine ligands are implicated as effective catalysts for formate dehydrogenation and exhibit sufficient air stability and recyclability. Avoiding troublesome additives and organic solvents lessens environmental impacts of the system and makes it more attractive from an economic point of view, while by-product formation is completely avoided. The absence of CO₂ both in the hydrogen storage step as well as the formate dehydrogenation stream further untangles the overall construction of a practical system. The utilization of highly concentrated aqueous cesium salt solutions enables the release of appreciable amounts of H₂ that have the potential to power real-world devices. The higher cost of cesium metal with respect to sodium and potassium constitutes a “capital” investment—as the material is recycled in situ, it does not add to the operating expenses of the proposed system. Finally, the presented system offers the possibility of controlling the H₂ output by simply adjusting the operating pressure. The effect of pressure has also been rationalized through identification of important intermediates of the catalytic mechanism.

Experimental Section

General considerations

All experiments were prepared without exclusion of air, however during heating a protective N₂ atmosphere was applied for reac-

tions performed under isobaric conditions. Recycling runs were also performed in air. {RuCl₂(*m*TPPTS)₂}₂ was prepared according to a literature procedure^[39] and checked for purity by ³¹P spectroscopy. All other chemicals are commercial products and were used without any further purification. CsOOCH (99%) was obtained from ChemPur, CsHCO₃ (99%) from ABCR, *m*TPPTS from Nanjing Chemlin Chemical Industry Co., Ltd, China. NaH¹³C and NaOO¹³CH (99% in ¹³C) were purchased from Cambridge Isotope Laboratories and H₂ (99.95%) was supplied by Carbogas-CH.

NMR spectroscopy

¹H, ¹³C, and ³¹P{¹H} NMR spectra were recorded on a Bruker Avance DRX 400 MHz (10 mm) spectrometer and the spectra processed with TopSpin, MestReNova and Matlab. Hydride-containing species were characterized by ¹H NMR spectroscopy using a water-suppression pulse sequence tuned to enhance the resulting spectrum in the upfield region.^[45] The *T*₁ values of hydride species were determined by a standard inversion recovery method, applying selective 90° and 180° pulses on the peak of interest. The integration area of the hydride peak was plotted as a function of the recovery delay time and fitted with a three parameter exponential curve.

Dehydrogenation experiments under isochoric conditions

Experiments were conducted in 10 mm high-pressure sapphire NMR tubes. In a typical experiment, {RuCl₂(*m*TPPTS)₂}₂ and *m*TPPTS were dissolved in 2 mL H₂O under aerobic conditions, followed by addition of the substrate. The reaction was initiated by heating the sapphire tube with an electric heating jacket or directly in the spectrometer. The reactions were followed by monitoring the pressure increase as a result of gas formation as a function of time with a pressure transducer connected to the tube by a high pressure capillary, either manually or with an in-house LabView 8.2 program with a NI USB 6008 interface, and/or in situ by ¹³C NMR spectroscopy. Formate conversion was calculated by comparison of the obtained reaction pressure to the theoretical maximum pressure resulting from 100% formate dehydrogenation and monitored by quantitative ¹³C NMR spectroscopy (Figure S13 in the Supporting Information). For the theoretical calculations of the maximum obtained pressure, it was considered that the volume of the solution does not change by dissolved H₂ gas. This was a good approximation because the solubility of dihydrogen in aqueous solutions is very low. At low concentrations, commercially available NaOO¹³CH was utilized instead of CsOOCH to facilitate analysis by ¹³C spectroscopy.

Dehydrogenation experiments under isobaric conditions

Experiments were conducted in Schlenk tubes. In a typical experiment, {RuCl₂(*m*TPPTS)₂}₂ and *m*TPPTS were dissolved in a 2 mL volume of H₂O under aerobic conditions, followed by addition of the substrate. Subsequently the tube was heated with an oil bath under a small N₂ overpressure. The produced H₂ gas was removed from the vessel with a needle placed through the rubber septum of the tube. If high-concentration CsOOCH solutions were decomposed, that is, prolonged heating was necessary, a condenser was connected to the tube to avoid evaporation of the solvent. After desired time intervals the tube was rapidly cooled down with water and the solution transferred to a 10 mm NMR tube for analysis.

Hydrogenation experiments

Catalytic bicarbonate hydrogenation experiments were performed either in 10 mm high-pressure sapphire NMR tubes or in 75 mL Parr autoclaves, which were the preferred option for experiments with high CsHCO₃ concentrations. In a typical experiment {RuCl₂(mTPPTS)₂}₂ and mTPPTS were dissolved in a 2 mL volume of H₂O under aerobic conditions, followed by addition of the substrate. The solution was then pressurized with H₂ up to the desired pressure and heated either with an electric heating jacket in case of sapphire tubes or with an oil bath in the case of autoclaves. Reactions in tubes were periodically monitored by quantitative ¹³C NMR spectroscopy. In the case of autoclaves, the reactor was cooled, depressurized, and then the aqueous solution was transferred to a standard 10 mm NMR tube for analysis. If samples containing both CsOOCH and CsHCO₃ were analyzed, with the latter close/over the room temperature solubility limit, sapphire tubes were pressurized with 60 bar H₂ to avoid CsOOCH decomposition and heated inside the spectrometer to ensure dissolution of CsHCO₃.

Recycling experiments

A 0.24 mol kg⁻¹ aqueous solution of NaH¹³CO₃ (2 mL H₂O) was pressurized with 100 bar H₂ in a sapphire tube, in the presence of 0.01 mol kg⁻¹ {RuCl₂(mTPPTS)₂}₂ and 2 equivalents mTPPTS. The tube was heated to 80 °C and the bicarbonate hydrogenation reaction followed by quantitative ¹³C NMR spectroscopy. Spectra of the sealed, pressurized solution were taken at regular time intervals until the equilibrium position was attained. Subsequently, the excess H₂ gas was vented, the tube sealed, and reheated to 80 °C under isochoric conditions and the formate dehydrogenation reaction followed by quantitative ¹³C NMR spectroscopy. Once the decrease in the formate concentration (and increase in the bicarbonate concentration) ceased, the tube was repressurized with 100 bar H₂ to initiate a new catalytic cycle. This procedure was repeated five times without taking precautions against air exposure or replenishing the solvent.

Acknowledgements

The authors are grateful to the Swiss National Science Foundation and EPFL for financial support. Dr. P. Miéville is thanked for valuable support with NMR techniques.

Keywords: cesium · dehydrogenation · hydrogenation · reaction mechanism · ruthenium

- [1] K. Mazloomi, C. Gomes, *Renewable Sustainable Energy Rev.* **2012**, *16*, 3024–3033.
- [2] N. Armaroli, V. Balzani, *ChemSusChem* **2011**, *4*, 21–36.
- [3] R. Williams, R. S. Crandall, A. Bloom, *Appl. Phys. Lett.* **1978**, *33*, 381–383.
- [4] B. Zaidman, H. Wiener, Y. Sasson, *Int. J. Hydrogen Energy* **1986**, *11*, 341–347.
- [5] D. C. Engel, G. F. Versteeg, W. P. M. van Swaaij, *Fluid Phase Equilib.* **1997**, *135*, 109–136.
- [6] C. Fellay, P. J. Dyson, G. Laurency, *Angew. Chem.* **2008**, *120*, 4030–4032.
- [7] B. Loges, A. Boddien, H. Junge, M. Beller, *Angew. Chem. Int. Ed.* **2008**, *47*, 3962–3965; *Angew. Chem.* **2008**, *120*, 4026–4029.
- [8] E. Graf, W. Leitner, *J. Chem. Soc. Chem. Commun.* **1992**, 623–624.
- [9] P. G. Jessop, T. Ikariya, R. Noyori, *Nature* **1994**, *368*, 231–233.
- [10] P. Munshi, A. D. Main, J. C. Linehan, C.-C. Tai, P. G. Jessop, *J. Am. Chem. Soc.* **2002**, *124*, 7963–7971.

- [11] R. Tanaka, M. Yamashita, K. Nozaki, *J. Am. Chem. Soc.* **2009**, *131*, 14168–14169.
- [12] T. J. Schmeier, G. E. Dobereiner, R. H. Crabtree, N. Hazari, *J. Am. Chem. Soc.* **2011**, *133*, 9274–9277.
- [13] Y. Himeda, N. Onozawa-Komatsuzaki, H. Sugihara, K. Kasuga, *Organometallics* **2007**, *26*, 702–712.
- [14] Y. Himeda, W.-H. Wang in *New Future Dev. Catal.* (Ed.: S. L. Suib), Elsevier, Amsterdam, **2013**, pp. 171–188.
- [15] W.-H. Wang, Y. Himeda, J. T. Muckerman, E. Fujita in *Adv. Inorg. Chem.* (Eds.: M. Aresta, R. van Eldik), Academic Press, **2014**, pp. 189–222.
- [16] G. Laurency, F. Joó, L. Nádasdi, *Inorg. Chem.* **2000**, *39*, 5083–5088.
- [17] J. Elek, L. Nádasdi, G. Papp, G. Laurency, F. Joó, *Appl. Catal. A* **2003**, *255*, 59–67.
- [18] S. S. Bosquain, A. Dorcier, P. J. Dyson, M. Erlandsson, L. Gonsalvi, G. Laurency, M. Peruzzini, *Appl. Organomet. Chem.* **2007**, *21*, 947–951.
- [19] C. Federsel, R. Jackstell, A. Boddien, G. Laurency, M. Beller, *ChemSusChem* **2010**, *3*, 1048–1050.
- [20] C. Federsel, A. Boddien, R. Jackstell, R. Jennerjahn, P. J. Dyson, R. Scopelitti, G. Laurency, M. Beller, *Angew. Chem. Int. Ed.* **2010**, *49*, 9777–9780; *Angew. Chem.* **2010**, *122*, 9971–9974.
- [21] R. Langer, Y. Diskin-Posner, G. Leitius, L. J. W. Shimon, Y. Ben-David, D. Milstein, *Angew. Chem. Int. Ed.* **2011**, *50*, 9948–9952; *Angew. Chem.* **2011**, *123*, 10122–10126.
- [22] G. Papp, J. Csorba, G. Laurency, F. Joó, *Angew. Chem. Int. Ed.* **2011**, *50*, 10433–10435; *Angew. Chem.* **2011**, *123*, 10617–10619.
- [23] A. Boddien, F. Gärtner, C. Federsel, P. Sponholz, D. Mellmann, R. Jackstell, H. Junge, M. Beller, *Angew. Chem. Int. Ed.* **2011**, *50*, 6411–6414; *Angew. Chem.* **2011**, *123*, 6535–6538.
- [24] A. Boddien, C. Federsel, P. Sponholz, D. Mellmann, R. Jackstell, H. Junge, G. Laurency, M. Beller, *Energy Environ. Sci.* **2012**, *5*, 8907–8911.
- [25] K. K. Turekian, K. H. Wedepohl, *Geol. Soc. Am. Bull.* **1961**, *72*, 175–192.
- [26] O.-T. Onsager, M. S. A. Brownrigg, R. Lødeng, *Int. J. Hydrogen Energy* **1996**, *21*, 883–885.
- [27] W. M. Haynes, T. J. Bruno, D. R. Lide, *Handbook of Chemistry and Physics*, CRC, Boca Raton, FL, **2014**.
- [28] R. C. Weast, *Handbook of Chemistry and Physics*, CRC, Boca Raton, FL, **1980**.
- [29] W. Ferguson, D. Gorrie in *Kirk-Othmer Encycl. Chem. Technol.*, John Wiley & Sons, Inc., New York, **2000**.
- [30] S. K. Howard, Society Of Petroleum Engineers, Richardson, TX, **1995**.
- [31] Cesium Formate Solution-Safety Data Sheet, Cabot Corporation, **2012**.
- [32] M. Zuvo, E. Bjornbom, B. Ellingsen, J. C. Downs, A. Kelley, H. C. Trannum, Society Of Petroleum Engineers, Richardson, TX, **2005**.
- [33] Y. Gilbert, P. Pessala, *Cs and Zn Comparative Hazard Assessment and HSE Profiles*, Gaia Consulting Ltd., Portage la Prairie, MB, **2012**.
- [34] C. Fellay, N. Yan, P. J. Dyson, G. Laurency, *Chem. Eur. J.* **2009**, *15*, 3752–3760.
- [35] K. Sordakis, M. Beller, G. Laurency, *ChemCatChem* **2014**, *6*, 96–99.
- [36] Q. Liu, L. Wu, S. Gülak, N. Rockstroh, R. Jackstell, M. Beller, *Angew. Chem. Int. Ed.* **2014**, *53*, 7085–7088; *Angew. Chem.* **2014**, *126*, 7205–7208.
- [37] A. Boddien, D. Mellmann, F. Gärtner, R. Jackstell, H. Junge, P. J. Dyson, G. Laurency, R. Ludwig, M. Beller, *Science* **2011**, *333*, 1733–1736.
- [38] A. Thevenon, E. Frost-Pennington, G. Weijia, A. F. Dalebrook, G. Laurency, *ChemCatChem* **2014**, *6*, 3146–3152.
- [39] M. Hernandez, P. Kalck, *J. Mol. Catal. A* **1997**, *116*, 117–130.
- [40] E. Fache, F. Senocq, C. Santini, J.-M. Basset, *J. Chem. Soc. Chem. Commun.* **1990**, 1776–1778.
- [41] Z. Tóth, F. Joó, M. T. Beck, *Inorg. Chim. Acta* **1980**, *42*, 153–161.
- [42] L. Helm, A. Borel, *NMRICMA 3.0*, ISIC EPFL, Lausanne, Switzerland, **2003**.
- [43] F. Joó, J. Kovács, A. C. Bényei, Á. Kathó, *Angew. Chem. Int. Ed.* **1998**, *37*, 969–970; *Angew. Chem.* **1998**, *110*, 1024–1026.
- [44] D. G. Hamilton, R. H. Crabtree, *J. Am. Chem. Soc.* **1988**, *110*, 4126–4133.
- [45] Bruker Program Library, p1331 Pulse Sequence for Water Suppression.
- [46] C. Bianchini, D. Masi, M. Peruzzini, M. Casarin, C. Maccato, G. A. Rizzi, *Inorg. Chem.* **1997**, *36*, 1061–1069.
- [47] S. Moret, P. J. Dyson, G. Laurency, *Dalton Trans.* **2013**, *42*, 4353–4356.

Received: April 1, 2015

Published online on June 26, 2015